Fibers and Polymers 2021, Vol.22, No.3, 793-803
DOI 10.1007/s12221-021-0512-1

ISSN 1229-9197 (print version)
ISSN 1875-0052 (electronic version)

Comparison of Static and Long-term Creep Behaviors between Balau Wood and Glass Fiber Reinforced Polymer Composite for Cross-arm Application

M. R. M. Asyraf[1]*, M. R. Ishak[1,2,3]*, S. M. Sapuan[3,4], and N. Yidris[1]

[1]*Department of Aerospace Engineering, Universiti Putra Malaysia, 43400 UPM Serdang, Selangor, Malaysia*
[2]*Aerospace Malaysia Research Centre, Universiti Putra Malaysia, 43400 UPM Serdang, Selangor, Malaysia*
[3]*Laboratory of Biocomposite Technology, Institute of Tropical Forestry and Forest Products, Universiti Putra Malaysia, 43400 UPM Serdang, Selangor, Malaysia*
[4]*Advanced Engineering Materials and Composites Research Centre, Department of Mechanical and Manufacturing Engineering, Universiti Putra Malaysia, 43400 UPM Serdang, Selangor, Malaysia*
(Received May 6, 2020; Revised June 10, 2020; Accepted June 14, 2020)

Abstract: Cross arms are mainly made up of wood (conventional) and pultruded glass fiber reinforced polymer composite (modern) installed in suspension tower. However, the creep response of both materials has not been fully covered in many literatures to explain the long-term durability of the current cross arm design. Thus, it is necessary to find the creep trends and models to evaluate the behavior in the tropical outdoor environment. The creep properties of Balau wood and pultruded composite at load of 10, 20 and 30 % of ultimate flexural stress were evaluated from quasi-static flexural test results. Using several creep numerical models, the creep properties of wood and composite cross arms were modelled. The results showed that the GFRP had a significant value of flexural strength, while Balau wood performed better in flexural modulus. In terms of creep properties, GFRP specimen exhibited high creep resistance with greater stability during transition from elastic to viscoelastic phase. From numerical modelling perspective, the simulated creep trends from Burger and Norton models were deviated from the experimental data. Subsequently, the most suitable creep model to forecast the creep behavior for wood and composite specimens was Findley model. All in all, pultruded composite is the most appropriate durable material to be applied in cross arms, while Findley model is a suitable model to represent creep performance of anisotropic materials.

Keywords: Cross arm, Glass fiber reinforced polymer composites, Balau wood, Flexural properties, Non-linear response

Introduction

Currently, modern urban areas consume around 75 % of power usage in order to perform the population's daily routine involving industrial and residential sectors [1]. Therefore, it is required for energy providers to supply electrical power to the consumers using high voltage transmission tower. Numerous parts of transmission line systems are constructed from continuous overhead power line cables and lifted via tall latticed steel structure tower [2, 3]. Most transmission towers are made up of galvanized steel, hardwood timber, and composite material as structural material with various designs and sizes. These towers accommodate electrical supply from 420 substations using three main operating lines, at 132, 275 and 500 kilovolts (kV) [4]. Generally, a transmission tower usually consists of structural joining members, which is incorporated in cross arms, tower body, cage, and peak. One of the crucial components of transmission tower is cross arm (Figure 1). It is an extended assembly of several long arm members used to lift and support electrical utility wire above the ground.

In 1963, cross arms in 132 kV suspension tower were built from Chengal wood. However, due to the limited supply of hardwood timber and wood aging degradation, it has led to the needs to find new alternatives [5,6]. Since the wooden cross arm is composed of natural fiber, it exhibits the characteristics of natural wood defects when exposed to continuous loading in a prolonged time in high humidity environment [7-12]. Thus, a research led by Rawi *et al*. [5] suggests that a comprehensive approach has to be taken to substitute wooden cross arms with other alternatives such as

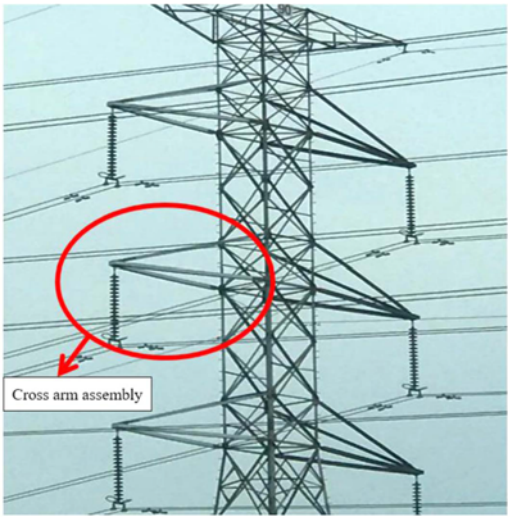

Figure 1. Application of cross arm assembly holding electrical cable and insulator in transmission tower.

*Corresponding author: asyrafriz96@gmail.com
*Corresponding author: mohdridzwan@upm.edu.my

glass fiber reinforced polymer (GFRP) composite material in the Malaysian electrical grid system. This has been attributed due to the combination of E-glass fiber with unsaturated polyester resin which displays a promising attributes, performance and manufacturability for heavy construction application [13]. Several studies show that the GFRP composite has been widely used in several structural industries including wind turbine, bridge deck, retrofitted beam and structural fastener [14-17]. This is due to the fact that the composite is made up of fine fiber which exhibits lightweight properties, stiff and high in mechanical strength with less raw material and production cost [18-21].

Since the pultruded GFRP composite is currently new to cross arm's application compared to hardwood timber, the study on long-term durability is not yet fully explored. In this case, it is essential to do a profiling on long-term mechanical testing (creep) in coupon scale to characterize this behavior in actual condition. A coupon scale experiment is performed to evaluate both wooden and composite cross arms using a three-point flexural mode. This creep test would evaluate the mechanical properties in terms of compression, tension, and shearing actions [13,22]. The bending effect in this mode can be moralized, and mimics the cantilever beam mode of the in-service cross arm in transmission tower [23]. The creep pattern obtained from both materials would provide better understanding, and can be further extended to predict their service life [20,24]. Thus, this creep study would establish a preliminary and comprehensive analysis for conventional (wood) and current (composite) cross arm's materials before extending to a full-scale cross arm structure.

To obtain significant creep results, a conventional mode of test (load based test) has to be conducted for a minimum of 1,000 hours. The creep trends obtained can be further elaborated and extended using available numerical modelling. Currently, there are two types of numerical models proposed in several literatures [25-28], such as physical (Burger model) and empirical (Findley power law and Bailey-Norton) models. These models aid researchers and engineers to predict the time-dependent long-term properties of the material either by implementing empirical formulation in terms of power-based approach or physical dashpot-spring element applications.

In this study, Balau wood was used to be compared with pultruded composite cross arm in the long-term mechanical test. Since Balau wood has similar mechanical and physical properties with Chengal wood [29] as well as cheaper and easily available in the market [30], it is suitable to be used in this experiment as a wooden cross arm representative. Balau or *Shorea Dipterocarpaceae* is a hardwood timber species originated from the South East Asia regions, especially densely located in Malaysia, Indonesia and the Philippines. It is commonly known as dense hardwood applied for heavy construction in buildings and bridges due to its high mechanical strength and stiffness (19.4 GPa of elasticity modulus and 142 MPa of rupture modulus). The texture of wood timber is moderately fine with interlocked grain to produce a figure of stripe on their radial surface. Balau hardwood is considered easy to manufacture and operate since it has comparatively low density to be managed (850-1155 kg/m^3) [31]. Thus, this explains Balau wood is suitable to represent conventional cross arms to be compared with pultruded GFRP composite for current cross arms.

In this manuscript, the goals of the project are to characterize and compare the quasi-static flexural and creep properties of Balau wood and pultruded GFRP composites in actual outdoor condition. Balau wood and GFRP composite exhibit better quality in terms of mechanical properties in various literatures [31,32], yet a comparative study on long-term mechanical properties of cross arm's laminated material is still not fully discovered. This study aids in estimating the quasi-static behaviors and creep trends in order to establish a verification on the existing cross arm's material which is very suitable in transmission tower application. Subsequently, it would provide a good view for readers to understand the impact of composite material in heavy construction applications such as in transmission line sector. Moreover, this article also highlights the verification of the applicability of the existing creep models to describe the creep strain of wood and composite cross arm in coupon scale size. Lastly, the paper also develops a general equation to predict creep response by using the best-fitting model.

Experimental

Around thirty-two (32) Balau wood and pultruded glass fiber reinforced polymer (GFRP) composite laminates were used in this project. Balau hardwood sample was obtained from Hang Tuah Sawmill Berhad, Negeri Sembilan,

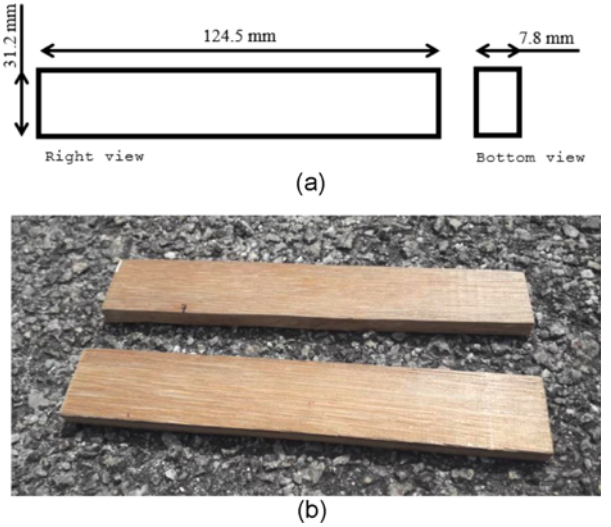

Figure 2. Schematic (a) and physical (b) coupon geometry.

Malaysia, while pultruded GFRP composite was obtained from Electrius Sendirian Berhad, Selangor, Malaysia. The average specimen size (Figure 2) was 7.8 mm in depth, 31.2 mm in width and 125 mm in span length. The samples were divided into two groups, which encompassed one (quasi-static flexural group) n=4 strips, and one (flexural creep group) n=12 strips. For the whole project, those specimens were subject to both quasi-static and long-term mechanical tests, which were explained as follows.

Properties of Balau Wood and Glass Fiber Reinforced Polymer Composite

The wood and composite specimens (Figure 2) were directly obtained from matured Balau timber trunk, into long plank shaped and single pultruded member of GFRP cross arms, respectively. Later, they were cut into rectangular shapes without any surface modification from both materials. The specifications of the Balau wood and pultruded GFRP composite such as density, texture, shrinkage, natural durability, rupture modulus and elastic modulus are listed in Table 1 [31,33,34]. In terms of pultruded GFRP composite compositions, fabric orientations and thickness aspect, they are described in Table 2.

Table 1. Properties of coupon strips [31,58,59]

Properties	Balau wood	Pultruded GFRP composite
Density	850-1155 kg/m^3	2580 kg/m^3 - E-glass 1350 kg/m^3 - Unsaturated polyester
Texture	Fine and even with deeply interlocked grain	Fine, homogenously and unidirectional fiber along the matrix
Shrinkage	High	Low
Natural durability	Very high	Low
Modulus of elasticity	20.1 GPa	29.8 GPa
Modulus of rupture	142.0 MPa	858.0 MPa

Table 2. Comprehensive information on composition, fabric orientation and thickness of pultruded GFRP composite [6,60]

Composition of pultruded GFRP composite		
Materials	Fiber	Resin
Pultruded GFRP composites	E-glass fiber (37 vol%)	Unsaturated polyester (UPE) (63 vol%)
Fabric orientation and thickness of pultruded GFRP composite		
GFRP composite layer	Fabric orientation (°)	Thickness (mm)
First (*Outer)*	45	0.5
Second	-45	0.5
Third	90	0.7
Forth	0	3.6
Fifth *(Inner)*	45	0.7

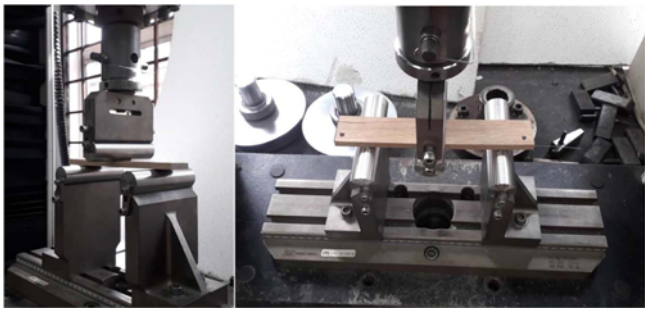

Figure 3. Quasi-static flexural test setting on rectangular coupons.

Quasi-static Flexural Test

The values of flexural strength and modulus for Balau and GFRP specimens were attained from an average of four repetitions in quasi-static flexural test. The test was conducted based on the international testing standard, ASTM D790. First, four samples from both Balau wood and GFRP composite were subject to short-term flexural tests, which used INSTRON Universal Testing Machine with 250 mm in diameter of supports and nose fixture. The loading speed of the flexural test was set to 3.33 mm/min to evaluate the bending properties for both materials under instantaneous loading effect. Figure 3 displays the quasi-static flexural test used to examine the quasi-static bending properties of wooden and composite specimens.

Flexural Creep Test

The creep test was conducted based on the international testing standard called ASTM D2990 focusing on flexural creep test. From the standard, four specimens were subject to long-term durability test for 1000 hours in an opened area.

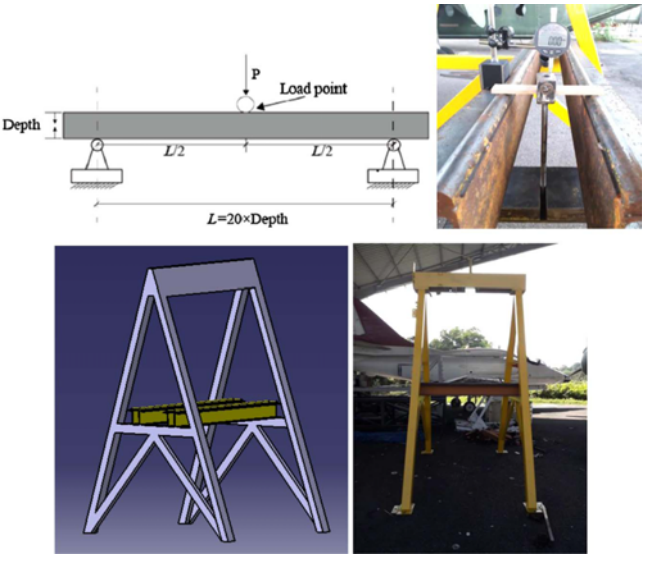

Figure 4. Schematic and actual experimental setup for flexural creep test for wooden and composite coupons.

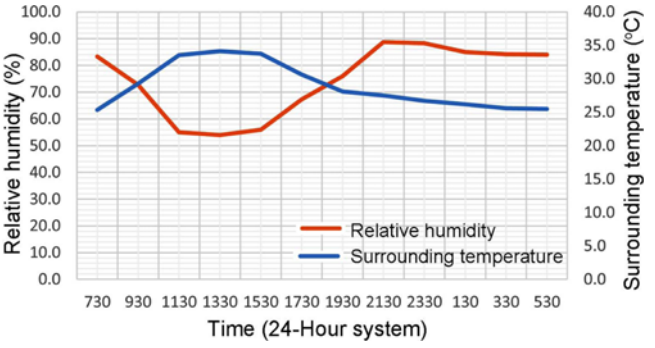

Figure 5. Average 24-hours of daily temperature and relative humidity.

It was conducted using custom test rig (Figure 4) in order to evaluate creep durability of the Balau wood cross arm's coupon strip in actual outdoor condition of the tropical season. The creep test assessed the mechanical strength of Balau wood and GFRP composite specimens under three load levels, as obtained from quasi-static flexural test. These loads were divided into three consecutive values, such as 10, 20 and 30 % from the ultimate flexural strength (UFS) of wood and composites, respectively. The deflection of each specimen was recorded using dial gauge for 1000 hours. The dial gauge was positioned at the top of the loading nose to measure the deflection value. The test took place from October to December 2019 (raining season), and hot weather was experienced in the afternoon, and it was raining in the evening. The daily relative humidity and temperature can be seen in Figure 5. Each specimen was kept for at least one month at room temperature before the test was conducted. All measurement instruments were calibrated before the test started.

These specimens were notated with alphabetical and numerical codes which are W, G, C and P, where W indicates Balau wood, G indicates pultruded GFRP composite, C indicates creep test, and P indicates the percentage value of the constant loading applied (10=10 % from ultimate flexural strength; 20=20 % from ultimate flexural strength; 30=30 % from ultimate flexural strength; 40=40 % from ultimate flexural strength). All specimens are noted in Table 3.

Table 3. Variation of creep loading for coupon specimens

Name	Test	Duration (hours)	Initial load (%)	No. of specimens	Load (N)
WC10	Creep	1000	10	4	203
WC20	Creep	1000	20	4	406
WC30	Creep	1000	30	4	609
WC40*	Creep	1000	40	4	812
GC10	Creep	1000	10	4	436
GC20	Creep	1000	20	4	872
GC30	Creep	1000	30	4	1308

Note: *Failure occurred after 200 hours of loading.

In terms of measuring instruments, dial gauges were used. To ensure the strain measuring tool was properly calibrated, the tool was compared with the analogue dial gauge during the strain evaluation. In this study, four different loads were implemented, which are 10, 20, 30 and 40 % from UFS. The specimens were experimented to study the creep as reported in Table 3. However, the strain-time graph at 40 % of load level was not described due to its failure after 200 hours of testing from the initial applied loading on the specimens. These tests clearly pointed out that a constant load at 40 % of load level caused creep rupture of the Balau hardwood rectangular coupon in more than 200 hours. Since the Balau wood only withstood 1,000 hours of creep operation up to 30 % of UFS, the same load levels were applied for pultruded composite, which are 10, 20 and 30 % of UFS.

The bending stress was applied with dead load in the middle of the strips from the initial time loading, t_0, which caused an instantaneous elastic strain. Nevertheless, some nominally equal tests were different. These differences were not subject to possible loss during calibration of the gauge with time as it was verified in the first place, neither from the inhomogeneity from the specimen stiffness, which was not observed during flexural test of the specimens of the same batch. This was due to loss of calibration during high speed of wind and seismic effect from external work from the surrounding areas. During the installation process, the specimens were operated manually using the lifter machine to hang the dead weight and the operating duration was within 15 minutes. A significant creep strain was induced due to load rate affecting the total deflection, which contributed to both creep and instantaneous elastic deformations.

Results and Discussion

Mechanical Behavior of Wooden and Composite Cross Arms

Figure 6 shows the flexural stress-strain curve of Balau wood and pultruded GFRP composite. The graph displays that the GFRP composite can withstand higher bending stress compared to Balau wood specimen. Moreover, it is interesting to note that the strain at failure for Balau wood is lower than GFRP composite. These results could be due to the delay of the breakage of glass fiber when the force was applied, which protected the composite laminate. The delay of the breakage of glass fiber occurred when macromolecular chain of unsaturated polyester (UPE) resin was more prospectively slipped and stretched in high elasticity rate [35,36]. As a result, the presence of UPE as a matrix in the composite laminate provided higher toughness and stiffness besides the compatibility of E-glass fiber and UPE resin. Overall, the trends of both wooden and composite specimens exhibited that the GFRP composite showed more

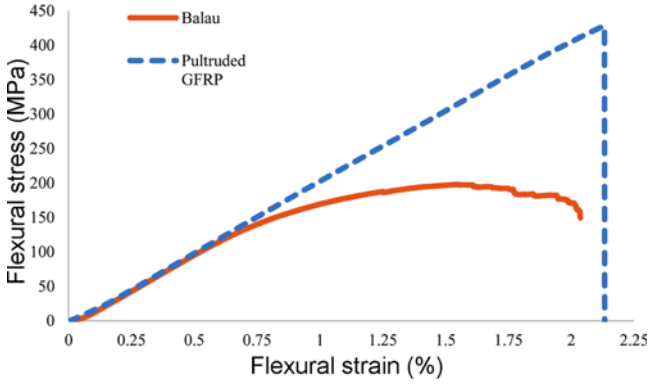

Figure 6. Flexural stress-strain curve of Balau wood and pultruded GFRP composite specimens.

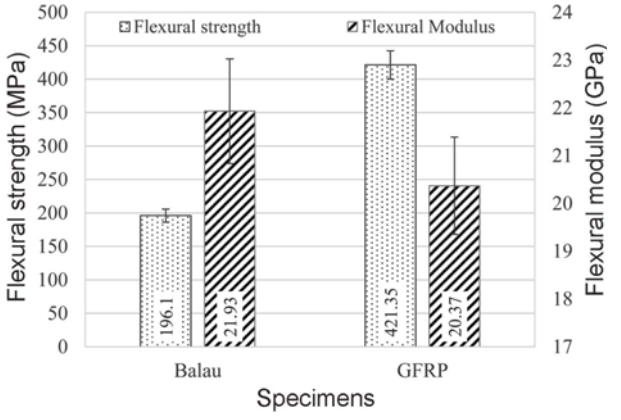

Figure 7. Flexural strength and modulus of Balau wood and pultruded GFRP composite.

brittle characteristic than Balau wood after ultimate flexural stress (UFS) was achieved.

According to Figure 7, the average elastic modulus of Balau wood was 21.93 GPa, and pultruded GFRP was 20.44 GPa. The average flexural strength for wood and composite found were about 196.1 MPa and 421.4 MPa, respectively. The elastic modulus of Balau wood was slightly higher by 7.1 % in relation to pultruded GFRP. This showed that both materials of wood and GFRP composite exhibited almost the same quality to resist the deformation elastically. However, the strength of the wood exhibited significantly lower by 73 % in relation to GFRP composite due to poor mechanical properties of hardwood related to GFRP composite [37]. The poor mechanical properties of wood resulted from composition of natural fiber which consisted of cellulose, hemicellulose, lignin, and pectin. These compositions allowed weak interaction among the fibers, which promoted internal defects and cracks. Subsequently, it induced to early crack development and growth [10,25,34,38].

From Table 4, it is found that the cross arm materials such as Balau wood and pultruded GFRP composite have higher quasi-static flexural performance compared to the previous materials tested. In terms of wooden material category, Balau wood has better bending strength and modulus compared to laminated veneer lumber (LVL), as Balau is considered hardwood timber [39], while Poplar veneer is a softwood, and it needs to be further enhanced via laminating and smearing by phenolic resin [40]. On the other part, pultruded GFRP composite applied in the experiment exhibited significantly greater bending properties compared to the glass fiber reinforced epoxy composite conducted by Zulkifli and Chow [41]. This could be due to the pultrusion process that aided the glass fiber to be fully wetted by resin to avoid void formation in composite laminate [42]. Hence, those two cross arm materials' bending properties (strength and modulus) have significant values to be used in heavy construction transmission applications.

Creep Trends and Properties

The strain-time graphs of the Balau wood and pultruded GFRP composite at three load levels are displayed in Figure 8. Both Balau and GFRP specimens were shown to increase creep strain as the load levels increased. From Figure 8, both curves revealed that there were two phases occurred during 1000 hours of creep operation, such as elastic and viscoelastic regions. As reported by Sanyang *et al*. [43], an anisotropic material such as wood and polymeric composite usually behaves elastically, followed by viscoelastic condition before entering plastic region. In this experiment, it seemed that the transition period from the elastic period to the constant viscoelastic state was extended in Balau wood as shown in the arrow as in Figure 8. This showed that the pultruded GFRP specimen experienced better stable viscoelastic state than conventional material for cross arm (Balau wood). Furthermore, the force implemented to the pultruded GFRP laminate was higher than the applied force to Balau wood at the same load level. This observation happened as GFRP

Table 4. Comparison of current experimental specimens and other research works materials in term of flexural properties

Type of materials	Experimental specimen and others related works	Specimen preparation	Flexural strength (MPa)	Flexural modulus (GPa)	Ref
Wooden material	Balau wood	Cutting (virgin timber)	196.10	21.93	[40]
	Laminated veneer lumber	Laminating (poplar veneer wood)	68.21	6.06	
GFRP composite	Pultruded glass fiber reinforced UPE composite	Pultrusion (fiber fabric ply)	421.35	20.37	[41]
	Glass fiber reinforced epoxy composite	Hand lay-up (chopped strand mat)	220.40	4.98	

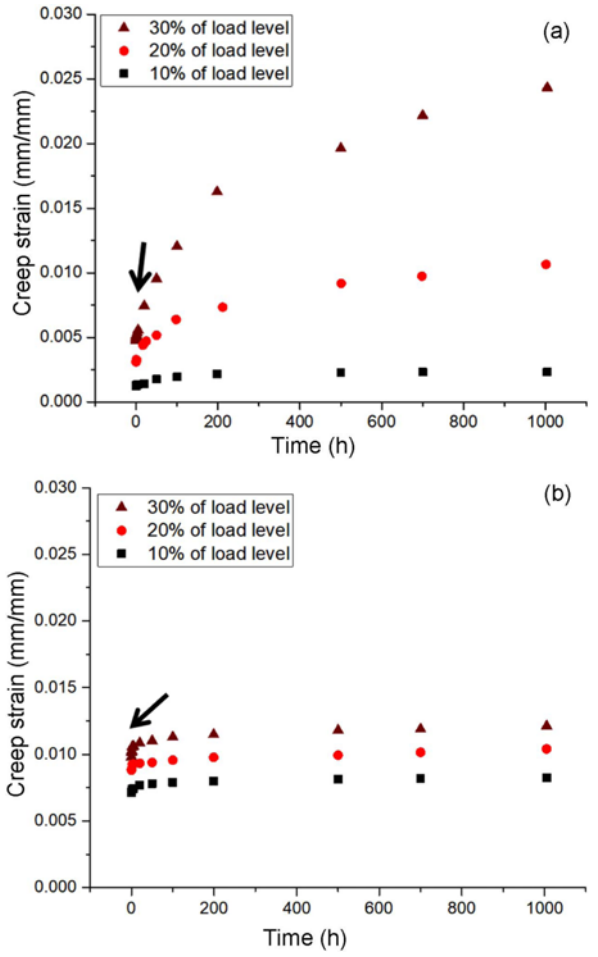

Figure 8. Comparison of creep strain between (a) Balau wood and (b) pultruded GFRP specimens at 10, 20 and 30 % of load levels.

composite containing E-glass fiber exhibited higher tensile properties [44], and UPE had good compatibility with glass fiber to ease the stress transfer, and subsequently promoting better bending performance [45].

The initial strain was evaluated at 15 seconds after loading the specific weight. The evaluation was done in order to classify the instantaneous strain level. Both wood and composite samples permitted the same elastic property as elastomer. Hence, the wooden material followed Hooke's law ($F=kx$; F is elastic force, expressed in N; k is the elastic coefficient, expressed in N/m; x is elastic deformation, expressed in mm), which describes the stress-strain relationship [46]. In general, the relationship can be expressed as in equation (1).

$$\sigma = E\varepsilon$$

where, σ is applied stress, ε is the elastic strain, and E is the elastic modulus. The elastic modulus was identified using equation (1) as displayed in Table 5. The average of elastic modulus of GFRP specimen was less than Balau wood, resulting in higher elastic strain of the GFRP specimen at the same load level.

Table 5. Hooke's law parameter of Balau wood and pultruded GFRP samples in term of instantaneous elastic stage

Material	Load levels (%)	σ (MPa)	ε (10^{-3})	E (GPa)	Average of E (GPa)
Balau wood	10	19.0	1.24	15.32	13.21
	20	38.2	3.10	12.32	
	30	57.3	4.78	11.98	
Pultruded GFRP	10	42.2	7.12	5.92	9.47
	20	84.5	8.81	9.59	
	30	126.7	9.81	12.90	

Creep Compliance

Creep compliance is a measurement which describes a long-term durability in terms of strain per constant stress. It can be simplified into a mathematical equation defined as $J(t)=\varepsilon(t)/\sigma_0$ (σ_0 is constant stress, in unit MPa, $\varepsilon(t)$ is time-based strain under applied constant stress, $J(t)$ is creep compliance, in unit MPa^{-1}). Figure 9 presents the time-dependent compliance of the Balau wood and pultruded GFRP samples.

The consistency of the outcome of creep compliance of Balau wood for four replication samples for each stress levels indicated the stability of creep performance of the material. Based on the results obtained, Balau wood compliance increased creep compliance pattern as the load level increased. This observation has been confirmed by Hoseinzadeh *et al*. [47] and Nakai *et al*. [48] where the increase of creep compliance can be attributed to the structure degradation of the cell wall components as the samples continuously experienced daily rainy and hot weather. This has caused micro-cracks between the fibers to propagate, and fiber pull-off would occur due to the increase of stress magnitude [3,21,49]. On the other hand, the pultruded GFRP specimen had significantly lower creep compliance than Balau wood based on three consecutive load levels. This was attributed due to the compatibility of E-glass fiber and synthetic resin (unsaturated polyester) [50, 51], as well as high tensile properties of E-glass fiber [52] which hindered the continuous deformation by the creep along the creep period. Referring back to Figure 7, the GFRP specimen had greater bending strength compared to Balau wood in order to reduce the primary creep. In general, the pultruded GFRP possesses better ability to decelerate the creep rate compared to Balau wood, subsequently providing longer service life for the material to sustain constant load.

Creep Numerical Models

To assess the time-dependent creep responses of the Balau and GFRP specimen on the basis of the flexural information,

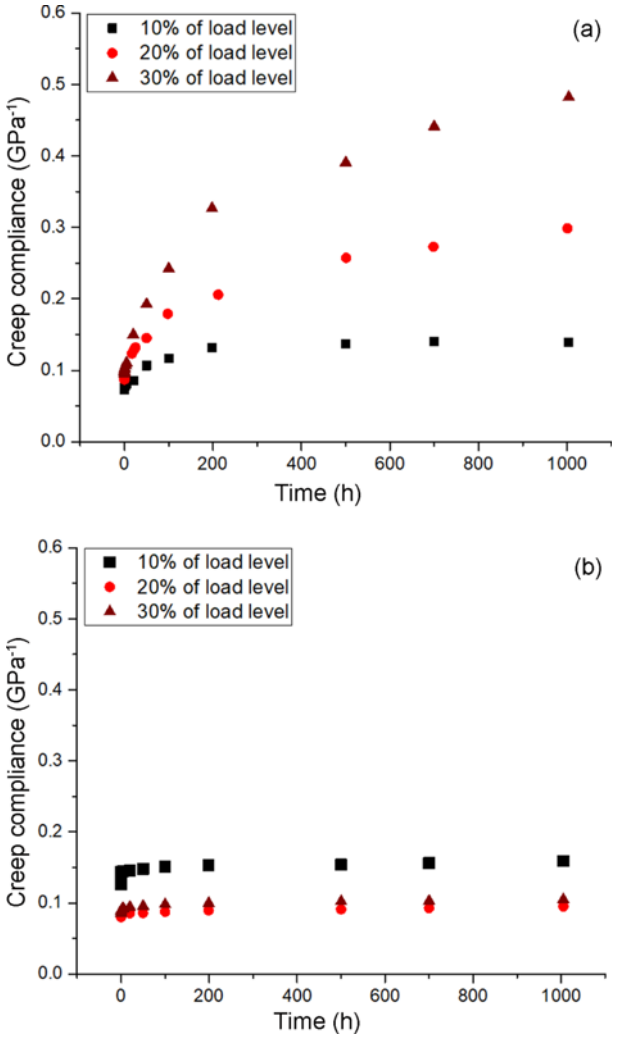

Figure 9. Creep compliance against time at different load levels for (a) virgin Balau wood and (b) pultruded GFRP specimens.

a reliable creep model has to be recognized. One of the models used in order to identify relationship between the material and creep properties via physical model is the Burger model [25,53]. This model can be expressed in equation (2).

$$\varepsilon(t) = \varepsilon_e + \varepsilon_d + \varepsilon_v$$

Total strain = Elastic strain + Permanent strain + Viscoelastic strain

$$\varepsilon(t) = \frac{\sigma}{E_e} + \frac{\sigma}{E_d}\left[1 - \exp\left(-\frac{E_d}{\eta_d}t\right)\right] + \frac{\sigma}{\eta_d}t$$

$$\varepsilon(t) = \varepsilon_0 + A[1 - \exp(-Bt)] + Ct \quad (2)$$

Equation (2) comprised of A, B, C and ε_0 as independent parameters. Hence, the model can be mentioned as four parametric variables. To be more accurate, both elastic and viscoelastic moduli are essential behavior of a material and can be elaborated using this model. Usually, these independent parameters (A, B, and ε_0) are linearly proportional to the applied stress, as well as C, which is supposed to be constant.

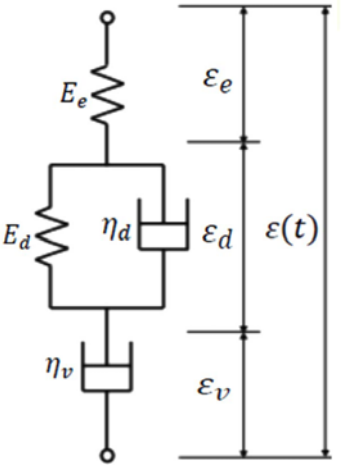

Figure 10. Schematic diagram of Burger model.

According to Perez *et al*. [54] and Chandra and Sobral [55], the Burger model comprised of a combination of three elements including a linear elastic spring, dash-pot and Kelvin-Voight element (a dash-pot and combination of dash-pot and spring). These elements explain the creep behavior in terms of elastic strain, permanent strain and viscoelastic strain. The stress usually responds at the tip of displacement and causes a strain to happen instantaneously. Figure 10 visualizes the long-term behavior of viscoelastic material under the Burger model.

Findley power law is an empirical mathematical model which simulates the creep behavior of anisotropic material. The model is presented as in equation (3) [56].

Total strain = Elastic strain + Transient strain

$$\varepsilon(t) = \varepsilon_0 + at^b \quad (3)$$

Equation (3) is made up of a and b as stress-dependent coefficient and stress-independent material constant, respectively. For instantaneous strain after exerting the load, it is represented and denoted as ε_0.

For Norton-Bailey law, it is considered as another empirical model to evaluate the primary and secondary creep under constant stress and temperature within the given time period. The model is expressed using equation (4) [26].

$$\varepsilon(t) = m\sigma^k t^n \quad (4)$$

where m, k, and n are classified as constants functions of temperature. In this project, the temperature parameter was selected as relatively constant. Hence, the equation (4) is deduced into equation (5) in order to predict the creep

properties under constant flexural stress.

$$\varepsilon(t) = Kt^n$$

where K can be attained using a non-linear fitting function in computer software, Origin 8.5, in order to organize the experiment data (creep strain and time) with three different stress values. The fitting was done by incorporating equation (5) in the mentioned modelling software. To be specific, the mean values of m and k can be determined using K. It can be derived by using the least-square curve fitting of the results of the flexural creep test.

Creep Model Validation

For this section, non-linear curve fitting was applied based on three models to acquire the mentioned parameters as discussed earlier. Figure 11 presents a comparison of creep strain-time curves between the stress levels of Balau wood

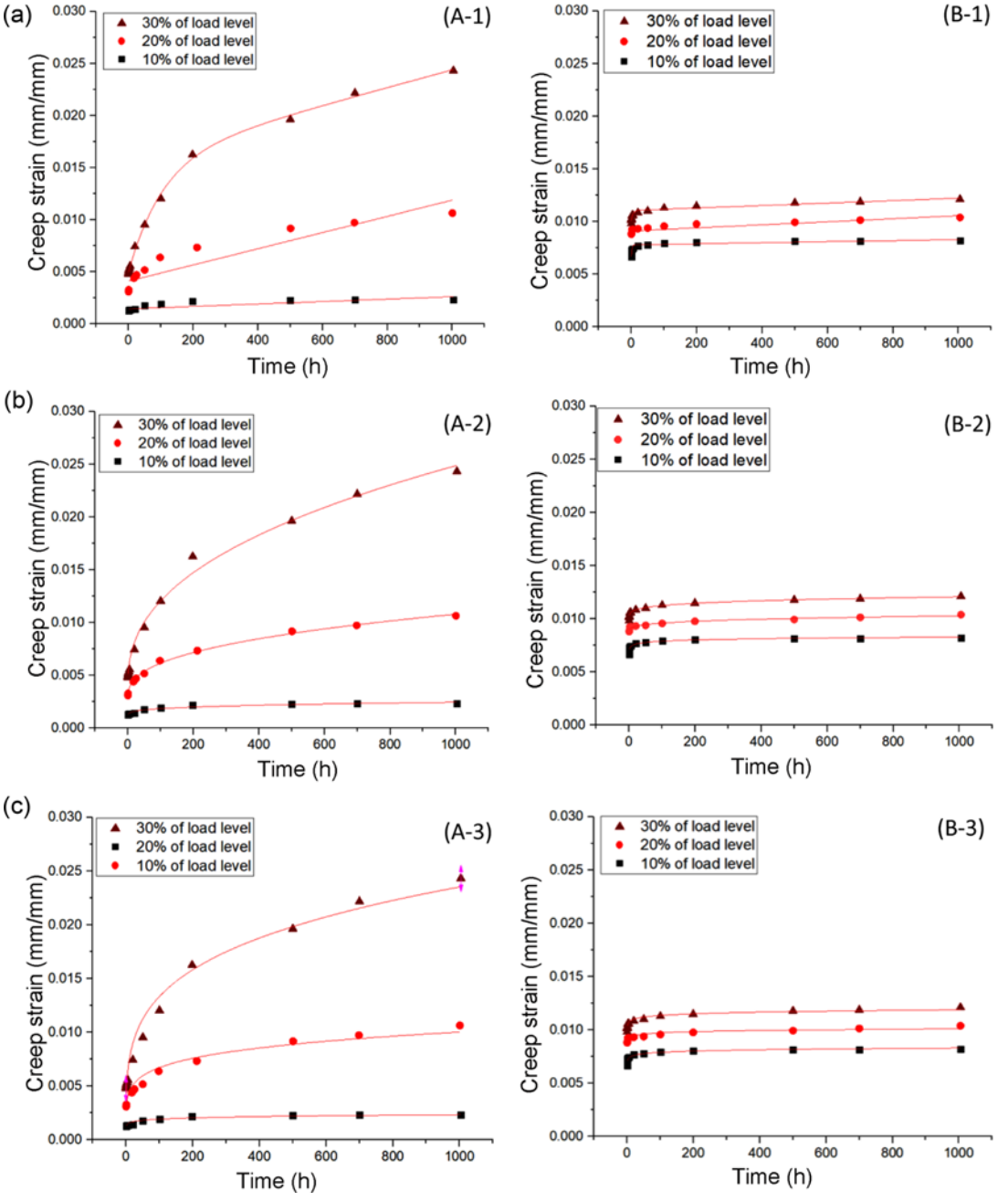

Figure 11. Experimental and modelled curve for three stress levels proportional to time in basis of (a) Burger model, (b) Findley model, and (c) Norton model.

Table 6. Overview of fitted parameters of Balau wood creep properties for three stress levels on the basis of the three models

Model	Parameter	Stress level (%)		
		10	20	30
Burger	ε_o	0.00146	0.00412	0.00506
	A	0	0	0.00857
	B	0	0	0.01087
	C	1.170×10^{-6}	7.775×10^{-6}	1.122×10^{-5}
	Adj. R^2	0.6156	0.8172	0.9944
Findley	ε_o	0.00108	0.00275	0.00427
	a	0.00025	0.00062	0.00089
	n	0.245	0.372	0.454
	Adj. R^2	0.9435	0.9968	0.9964
Norton-simplify	K	0.00133	0.0030	0.0042
	n	0.08184	0.1733	0.2492
	Adj. R^2	0.9069	0.9411	0.9539

Table 7. Overview of fitted parameters of pultruded GFRP laminate creep properties for three stress levels on the basis of the three models

Model	Parameter	Stress level (%)		
		10	20	30
Burger	ε_o	0.00742	0.00911	0.01008
	A	1.552×10^{-22}	1.645×10^{-22}	9.806×10^{-4}
	B	0	0	0.2012
	C	1.386×10^{-6}	1.466×10^{-6}	1.170×10^{-6}
	Adj. R^2	0.7189	0.7337	0.9503
Findley	ε_o	0.00698	0.00868	0.00972
	a	3.1122×10^{-4}	3.0768×10^{-4}	6.4318×10^{-4}
	n	0.234	0.240	0.189
	Adj. R^2	0.9953	0.9629	0.9930
Norton-simplify	K	0.00731	0.00901	0.01040
	n	0.0195	0.0165	0.0194
	Adj. R^2	0.9406	0.9118	0.9549

and pultruded GFRP specimens. The analysis and comparison results from fitted parameter from three consecutive models are simplified in Tables 6 and 7.

Based on Figure 11, the adjusted regression (adj. R^2) of the Burger model showed that Balau wood (A-1) had higher value than pultruded GFRP (B-1). This was attributed due to the fitting results for Balau wood samples which were better than pultruded composite samples. The Burger model fitted poorly for the pultruded GFRP samples when fitting the experimental data at the commencement period. The forecasted instantaneous strain was considered slightly more than the actual experimental creep data. This happened due to the model itself which estimated the creep behavior using a linear relationship between time and viscosity [23,25]. Apart from that, the composite samples showed that the creep rate steadily decreased along the 1,000-hour period of operation. Hence, the D value could be assumed as a dependent variable which was time rather than a constant value in this model [57].

Power law model is divided into Findley and Norton models, also known as empirical models. Previous studies state that both power models satisfy the steady-state creep behavior within a particular time period in order to elaborate the transient creep period [24,28]. According to Figure 11 (A-2, B-2, A-3 and B-3), the finding revealed that the fitting results of the Norton model were quite higher compared to the experimental data. However, for a longer duration, the model performed in a downward deviation from the experimental results. Among the simulated creep model, the best model to forecast the experiment data was Findley power model, where the adj. R^2 of the Balau wood (0.9968-0.9435) and pultruded GFRP (0.9930-0.9629) were the highest values. The fitting outcomes for the early stage of the Norton-Bailey model was greater than experimental results. The Norton's creep estimation deviated downwards from the experimental outcomes. On the basis of the fitting results based on these models, the long-term creep properties of Balau wood and GFRP samples were predicted by using Findley model to formulate a mathematical equation.

Creep General Equation

The creep validation of these two general equations were carried out by comparing the instantaneous strain from experimental data and Findley's model. Moreover, estimation of creep strain is also being simulated within their service life for further verification. The instantaneous elastic strain, ε_0, was directly proportional to the applied stress value according to equation (1). As depicted in Table 8, it contained the comparison of instantaneous elastic strain value between experimental data and Findley model for both Balau wood and pultruded GFRP laminates.

The findley model was implemented to forecast the creep behaviors of Balau wood and pultruded GFRP samples under 10, 20 and 30 % of ultimate flexural stress. In general, both samples can be generalized using mathematical equations in order to estimate their creep properties as in Table 9. The general equations for both Balau wood and

Table 8. Comparison of instantaneous elastic strain value between Findley model and experimental data

Specimen	Model	Instantaneous strain	Stress level (%)		
			10	20	30
Balau wood	Experimental data	$\varepsilon(10^{-3})$	1.24	3.10	4.78
	Findley model	$\varepsilon_0(10^{-3})$	1.08	2.75	4.27
Pultruded GFRP	Experimental data	$\varepsilon(10^{-3})$	7.12	8.81	9.81
	Findley model	$\varepsilon_0(10^{-3})$	6.98	8.68	9.72

Table 9. List of equations for specific stress level

Sample	Equation to forecast the creep response
Balau wood	$\varepsilon(t) = 5.87(10^{-4})t^{0.357} + \frac{\sigma}{E}$
Pultruded GFRP	$\varepsilon(t) = 4.21(10^{-4})t^{0.221} + \frac{\sigma}{E}$

pultruded GFRP are generated from Findley's power law model due to adjusted regression of the model is highest and have a good approximation for the creep properties of pultruded GFRP composite under tropical environment.

Conclusions and Recommendations

Wood and pultruded composite are common materials applied for cross arm structure in the transmission line tower. The quasi-static mechanical and creep behaviors of both Balau wood and pultruded GFRP composite were evaluated and analyzed. Generally, the modulus of elasticity of pultruded GFRP decreases by 7.09 % compared to Balau wood. In contrast, the flexural strength of pultruded GFRP increases about 72.97 % compared to Balau wood. Moreover, the pultruded GFRP exhibits higher instantaneous elastic deformation, and also indicates steady-state viscoelastic phase in early stage of creep at the same stress level. In this case, the creep strain rates and compliance of pultruded GFRP are elevated at viscoelastic stage which displays better creep resistance due to higher strength and fracture toughness of glass fiber. Apart from that, due to pultrusion process of E-glass fiber with unsaturated polyester, it provides better consistency and coherence of fiber reinforcement in composite laminate. Subsequently, pultruded GFRP performs more stable creep properties. Therefore, pultruded GFRP composite is very suitable as durable material to be applied and implemented as cross arm structure.

This study has verified the implementation of several creep models, such as Burger model, Findley power law model and Norton-Bailey model, in describing the creep behaviors of both wood and composite materials. The simulated results from these models also define the adjusted regression of (Adj R^2) using non-linear fitting method. According to the findings, it is depicted that the fitting curves from Burger and Norton-Bailey models are diverged obviously from the experimental outcomes at the end of the experiment. Thus, the numerical results have confirmed that Findley model is the optimized model to simulate the creep properties of both materials. All in all, two mathematical formulas (Balau wood and pultruded GFRP) have been derived from Findley model in order to forecast their creep properties.

Acknowledgements

The authors would like to thank Universiti Putra Malaysia (UPM) for the financial support provided through Geran Putra, UPM with VOT no. 9634000. The authors are very thankful to Department of Aerospace Engineering, Faculty of Engineering, UPM for providing space and facilities for the project. Moreover, all authors are very appreciate and thankful to Jabatan Perkhidmatan Awam (JPA) and Kursi Rahmah Nawawi for providing scholarship award and financial aids to the first author to carry out this research project.

References

1. S. S. S. Ali, M. R. Razman, and A. Awang, *Int. J. Energy Econ. Policy*, **10**, 84 (2020).
2. M. R. M. Asyraf, M. R. Ishak, S. M. Sapuan, and N. Yidris, *J. Mater. Res. Technol.,* **8**, 5647 (2019).
3. M. R. M. Asyraf, M. R. Ishak, S. M. Sapuan, N. Yidris, R. A. Ilyas, M. Rafidah, and M. R. Razman, *Adv. Civ. Eng.*, **2020**, 6980918 (2020).
4. M. S. A. Bakar, D. Mohamad, Z. A. M. Ishak, Z. M. Yusof, and N. Salwi, *AIP Conf. Proc.*, **2031**, 020027 (2018).
5. I. M. Rawi, M. S. A. Rahman, M. Z. A. Ab Kadir, and M. Izadi, International Conference on Power Systems Transients, 2017.
6. S. Beddu, A. Syamsir, Z. Arifin, and M. Ishak, *AIP Conf. Proc.*, **020039** (2018).
7. H. Peng, J. Jiang, J. Lu, and J. Cao, *J. Wood Sci.*, **63**, 455 (2017).
8. F. Segovia, P. Blanchet, A. Laghdir, and A. Cloutier, *Int. Wood Prod. J.*, **4**, 225 (2013).
9. R. A. Ilyas, S. M. Sapuan, A. Atiqah, R. Ibrahim, H. Abral, M. R. Ishak, E. S. Zainudin, N. M. Nurazzi, M. S. N. Atikah, M. N. M. Ansari, M. R. M. Asyraf, A. B. M. Supian, and H. Ya, *Polym. Compos.*, **41**, 459 (2020).
10. C. N. A. Jaafar, M. A. M. Rizal, and I. Zainol, *Int. J. Eng. Technol.*, **7**, 258 (2018).
11. M. R. M. Asyraf, M. R. Ishak, S. M. Sapuan, and N. Yidris, *J. Mater. Res. Technol.*, **9**, 2357 (2020).
12. R. A. Ilyas, S. M. Sapuan, A. Atiqah, M. R. M. Asyraf, R. S. Ayu, H. A. Aisyah, N. M. Nurrazzi, and M. N. F. Norrahim, *Text. Res. J.*, **91**, 152 (2021).
13. A. N. Johari, M. R. Ishak, Z. Leman, M. Z. M. Yusoff, and M. R. M. Asyraf, *Polimery*, **65**, 792 (2020).
14. Parikh, Kaushal, and C. D. Modhera, *Int. J. Civ. Struct. Eng.*, **2**, 1070 (2012).
15. J. Zhu and M. M. Lopez, *Compos. Struct.*, **113**, 108 (2014).
16. F. Lambiase, M. Durante, and A. Di Ilio, *J. Mater. Process. Technol.*, **236**, 241 (2016).
17. A. N. Johari, M. R. Ishak, Z. Leman, M. Z. M. Yusoff, M. R. M. Asyraf, W. Ashraf, and H. K. Sharaf, Seminar Enau Kebangsaan, 983, 2019.
18. A. Atiqah, M. Jawaid, S. M. Sapuan, M. R. Ishak, M. N. M. Ansari, and R. A. Ilyas, *J. Mater. Res. Technol.*, **8**, 3732 (2019).

19. P. Wambua, J. Ivens, and I. Verpoest, *Compos. Sci. Technol.*, **63**, 1259 (2003).
20. M. R. M. Asyraf, M. R. Ishak, S. M. Sapuan, N. Yidris, A. N. Johari, W. Ashraf, H. K. Sharaf, M. Chandrasekar, and R. Mazlan, Seminar Enau Kebangsaan, 38, 2019.
21. M. R. M. Asyraf, M. Rafidah, M. R. Ishak, S. M. Sapuan, R. A. Ilyas, and M. R. Razman, *Polym. Compos*., **41**, 2917 (2020).
22. V. Fiore, A. Valenza, and G. Di Bella, *J. Compos. Mater.*, **46**, 2089 (2012).
23. M. R. M. Asyraf, M. R. Ishak, S. M. Sapuan, N. Yidris, R. M. Shahroze, A. N. Johari, M. Rafidah, and R. A. Ilyas, *J. Mech. Eng. Sci*., **14**, 6869 (2020).
24. M. R. M. Asyraf, M. R. Ishak, M. R. Razman, and M. Chandrasekar, *J. Teknol.*, **81**, 155 (2019).
25. M. R. M. Asyraf, M. R. Ishak, S. M. Sapuan, N. Yidris, and R. A. Ilyas, *J. Mater. Res. Technol*., **9**, 6759 (2020).
26. D. L. May, A. P. Gordon, and D. S. Segletes, ASME Turbo Expo 2013: Turbine Technical Conference and Exposition, V07AT26A005, 2013.
27. Z. Yang, H. Wang, X. Ma, F. Shang, Y. Ma, Z. Shao, and D. Hou, *Compos. Struct.*, **193**, 154 (2018).
28. S. Siengchin, *J. Thermoplast. Compos. Mater.*, **26**, 863 (2013).
29. Annual Report 2018; Forestry Department of Peninsular Malaysia, Kuala Lumpur, Malaysia, 2018.
30. Aathaworld, Balau and Chengal supply in Malaysia, https://www.aathaworld.com/single-post/Balau-Chengal-Timber-Wood-Supplier-Malaysia (Accessed May 19, 2020).
31. Malaysian Timber Council, Balau Wood Technical Information, http://www.mtc.com.my/resources-WoodWizard.php (Accessed May 19, 2020).
32. T. P. Sathishkumar, S. Satheeshkumar, and J. Naveen, *J. Reinf. Plast. Compos.*, **33**, 1258 (2014).
33. V. S. Chevali, D. R. Dean, and G. M. Janowski, *Compos. Part A Appl. Sci. Manuf.*, **40**, 870 (2009).
34. N. M. Nurazzi, A. Khalina, S. M. Sapuan, and R. A. Ilyas, *Polimery*, **64**, 12 (2019).
35. A. M. N. Maisara, R. A. Ilyas, S. M. Sapuan, M. R. M. Huzaifah, N. M. Nurazzi, and S. O. A. Saifulazry, *Int. J. Recent Technol. Eng.*, **8**, 510 (2019).
36. N. M. Nurazzi, A. Khalina, S. M. Sapuan, R. A. Ilyas, S. A. Rafiqah, and Z. M. Hanafee, *J. Mater. Res. Technol.*, **9**, 1606 (2020).
37. S. D. Pandita, X. Yuan, M. A. Manan, C. H. Lau, A. S. Subramanian, and J. Wei, *J. Reinf. Plast. Compos.*, **33**, 14 (2014).
38. M. S. N. Atikah, R. A. Ilyas, S. M. Sapuan, M. R. Ishak, E. S. Zainudin, R. Ibrahim, A. Atiqah, M. N. M. Ansari, and R. Jumaidin, *Polimery*, **64**, 27 (2019).
39. M. D. Jantan and M. K. Tam, *Malaysian For.*, **48**, 159 (1985).
40. H. Fu, M. Dun, H. Wang, W. Wang, R. Ou, Y. Wang, T. Liu, and Q. Wang, *Constr. Build. Mater.*, **237**, 117499 (2020).
41. N. H. M. Zulfli and W. S. Chow, *J. Phys. Sci.*, **21**, 41 (2010).
42. A. M. Fairuz, S. M. Sapuan, E. S. Zainudin, and C. N. A. Jaafar, *Am. J. Appl. Sci.*, **11**, 1798 (2014).
43. M. L. Sanyang, S. M. Sapuan, M. Jawaid, M. R. Ishak, and J. Sahari, *BioResources*, **11**, 4134 (2016).
44. M. H. Hamidon, M. T. H. Sultan, A. H. Ariffin, and A. U. M. Shah, *J. Mater. Res. Technol.*, **8**, 3327 (2019).
45. D. Cho, H. S. Lee, and S. O. Han, *Compos. Interfaces*, **16**, 711 (2009).
46. H. W. Liu, "Mechanics of Materials", China Machine Press, Beijing, 2004.
47. F. Hoseinzadeh, S. M. Zabihzadeh, and F. Dastoorian, *Constr. Build. Mater.*, **226**, 220 (2019).
48. T. Nakai, K. Toba, and H. Yamamoto, *J. Wood Sci.*, **64**, 745 (2018).
49. R. M. Shahroze, M. Chandrasekar, K. Senthilkumar, T. Senthilmuthukumar, M. R. Ishak, and M. R. M. Asyraf, Seminar Enau Kebangsaan, 52, 2019.
50. A. Anand, P. Banerjee, R. K. Prusty, and B. Chandra Ray, *IOP Conf. Ser. Mater. Sci. Eng.*, 338 (2018).
51. D. W. Scott and A. H. Zureick, *Compos. Sci. Technol.*, **58**, 1361 (1998).
52. C. N. A. Jaafar, I. Zainol, and M. A. M. Asyraf, 27th Scientific Conference of Microscopy Society Malaysia 2018 (SCMSM2018), 5, 2018.
53. J. F. Hunt, H. Zhang, and Y. Huang, *BioResources*, **10**, 3131 (2015).
54. C. J. Pérez, V. A. Alvarez, and A. Vázquez, *Mater. Sci. Eng. A*, **480**, 259 (2008).
55. P. K. Chandra and P. J. do A. Sobral, *Ciência e Tecnol. Aliment.*, **20**, 250 (2006).
56. W. N. Findley, J. S. Lai, K. Onaran, and R. M. Christensen, *J. Appl. Mech*., **44**, 364 (1977).
57. M. Moutee, M. Fafard, Y. Fortin, and A. Laghdir, *Wood Fiber Sci.*, **37**, 521 (2005).
58. M. S. EL-Wazery, M. I. EL-Elamy, and S. H. Zoalfakar, *Int. J. Appl. Sci. Eng.*, **14**, 121 (2017).
59. G. Gündüz, D. Erol, and N. Akkaş, *J. Compos. Mater.*, **39**, 1577 (2005).
60. D. Mohamad, A. Syamsir, S. Beddu, A. Abas, F. C. Ng, M. F. Razali, and S. A. H. A. Seman, *IOP Conf. Ser. Mater. Sci. Eng.*, **530**, 012027 (2019).